DOI 10.1007/s005310000151

ORIGINAL PAPER

Susan Ellis · Silke Wissing · Adrian Pfiffner

Strain localization as a key to reconciling experimentally derived flow-law data with dynamic models of continental collision

Received: 14 July 1999 / Accepted: 9 October 2000 / Published online: 7 December 2000

Abstract Published strength profiles predict strength discontinuities within and/or at the base of continental crust during compression. We use finite element models to investigate the effect of strength discontinuities on continental collision dynamics. The style of deformation in model crust during continued subduction of underlying mantle lithosphere is controlled by: (1) experimental flow-law data; (2) the crustal geotherm; (3) strain localization by erosion; (4) strain-softening and other localization effects. In the absence of erosion and other factors causing strain localization, numerical models with typical geothermal gradients and frictional/ductile rheologies predict diffuse crustal deformation with whole-scale detachment of crust from mantle lithosphere. This prediction is at odds with earlier model studies that only considered frictional crustal rheologies and showed asymmetric, focused crustal deformation. Without localization, model deformation is not consistent with that observed in small collisional orogens such as the Swiss Alps. This suggests that strain localization by a combination of erosion and rheological effects such as strain softening must play a major role in focusing deformation, and that strength profiles derived under constant strain rates and uniform material properties cannot be used to infer crustal strength during collision dynamics.

Keywords Continental collision · Flow-laws · Numerical models · Rheology · Strength profiles

S. Ellis (✉) · S. Wissing · A. Pfiffner
Geologisches Institut, Universität Bern, Baltzerstrasse 1, Bern 3012, Switzerland
E-mail: s.ellis@gns.cri.nz
Phone: +41-31-6314738
Fax: +41-31-6314843

Present address:
S. Ellis
Institute of Geological and Nuclear Sciences, Lower Hutt, New Zealand

Introduction

A common approach when studying deformation of continental rocks is to use representative rheologies, geotherms and strain rates to estimate the strength of the crust. Rheological parameters derived from laboratory experiments for frictional behaviour (e.g. Amontons–Byerlees Law) and/or ductile flow (e.g. power-law creep) are extrapolated to crustal conditions to construct strength profiles such as the examples shown in Fig. 1. In general, they show the presence of one or more relatively weak horizons within and/or at the base of the crustal layer, giving rise to the characteristic 'Christmas tree' shape. Profiles differ depending on the assumed constitutive relations, the dominant mineral composition of various layers, and the temperature and density structure of the crust (see review by Kohlstedt et al. 1995). Such strength profiles have been used by many authors to interpret the behaviour of continental crust under compression.

An alternative approach is to consider the effect of lithospheric strength on dynamic behaviour of the crust or lithosphere using forward-model experiments. Materials such as sand or plasticine have been used within appropriately scaled analogue experiments to infer behaviour of crustal rocks. Rheological behaviour in the equivalent numerical experiments is represented by a series of constitutive equations relating stresses to strain and strain rates. In general, these experiments show large variations in strain-rate as a function of position and time (e.g. Albert et al. 2000). These variations bring into doubt the validity of strength profiles constructed from simple kinematic assumptions.

In this paper we highlight some of the problems in interpreting continental collision in terms of crustal strength profiles based on experimental data, by comparing them to strength profiles computed from a series of simple numerical experiments. We show that,

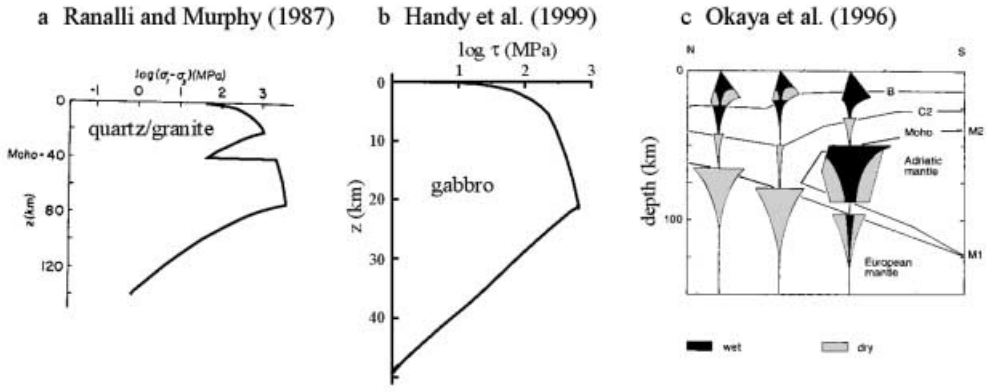

Fig. 1 Typical strength profiles predicted for continental crust taken from the literature. **a** 40-km-thick quartz/granite one-layer crust overlying an olivine mantle, with a linear 10 °C km^{-1} geothermal gradient and a constant strain rate of 10^{-14} s^{-1} (Ranalli and Murphy 1987). **b** 50-km-thick crust with a two- mineral phase gabbro composition (30% feldspar, 70% clinopyroxene) calculated using a bimineralic flow-law with interconnected, weak-layer mylonitic behaviour and a geothermal gradient of 20 °C km^{-1}. Simplified from Handy et al. (1999). Strain rate was constant at 10^{-12} s^{-1}. **c** Strength versus depth profiles constructed for the Central Alps from Okaya et al. (1996) using heat flow data and an assumed layered composition of quartzite/granite (upper crust); quartz–diorite (mid-crust, above C2 which is the Conrad discontinuity); diabase (lower crust, below C2 and above Moho); and olivine (mantle lithosphere). *Black* and *grey shading* show profiles for wet and dry rheologies, respectively. Profiles are computed for extension (*left-hand side*) and compression (*right-hand side*) using Byerlee's Law in the frictional domain. Constant strain rate of 10^{-15} s^{-1}

in general, localization of deformation by strain softening or erosion is required to reconcile dynamic model results with observations.

Dynamics of continental collision

Introduction and background

Results from geophysical surveys in small collisional orogens such as the Swiss Alps show an asymmetric geometry with lower crust and mantle lithosphere underthrusting the collision zone (e.g. Central Swiss Traverse; Fig. 2a). In the Alps, European lower crust remained coupled to the mantle, subducting beneath the Adriatic plate and causing a doubling in the Moho (Ye 1992), whereas in the eastern Swiss Alps, lower crust on the Adriatic plate was thickened and involved in the deformation (Pfiffner and Hitz 1997). In both central and eastern sections, little detachment at the Moho is inferred for the European plate (Schmid 1999), unlike dynamic predictions inferred from typical 'Christmas tree' strength profiles with a marked strength discontinuity at the base of the crust.

The asymmetric doubly vergent pattern observed in the European Alps and many other collision zones has been reproduced in a series of analogue experiments

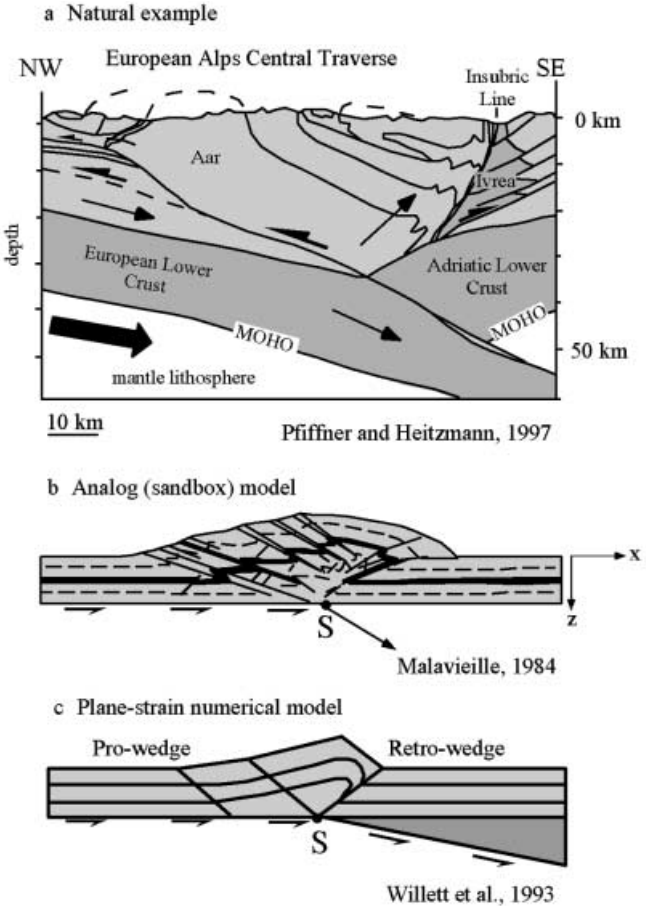

Fig. 2 Style of continental collision when crustal deformation is forced by subduction of lower lithosphere. **a** Interpreted dynamics and crustal deformation for the Swiss Central Traverse, modified after Pfiffner and Heitzmann (1997). *Dark grey* is lower crust. **b** Analogue sandbox experiment by Malavieille (1984). Lower lithosphere kinematics represented by Mylar sheet pulled along and through a slot at point *S*. Layers in sand are marker horizons; sand has uniform composition. **c** Equivalent finite-element numerical model experiment by Willett et al. (1993). Uniform crustal layer has frictional (Coulomb) properties. Lower lithosphere subduction is represented by the velocity boundary condition on the base, with an imposed velocity discontinuity at point *S*

(Malavieille 1984; Fig. 2b) with crustal layers represented by a frictional Coulomb material (sand) and the subduction of lower lithosphere by a mylar sheet pulled along and down through a slot at the point of collision. The sandbox experiments clearly show the influence of the lower lithosphere kinematics on deformation in the modelled layer above. A characteristic asymmetric deformation pattern develops, with plug uplift along two inclined shear zones on either side of the slot. Shear remains focused on the stationary side of the model orogen (the retro-side in the terminology of Willett et al. 1993), but is distributed in a series of outward-propagating thrust faults within the sand layer on the incoming (pro-) side. The same boundary conditions applied to a numerical model with a frictional rheology produce similar results (e.g. Willett et al. 1993; Fig. 2c), although the continuum assumptions used in the numerical model and the limited resolution of the finite elements causes shear zones to have a larger width than equivalent sandbox experiments. Lack of strain localization effects in numerical experiments also prevents the pro-wedge from developing as a series of discrete thrust planes; instead, it thickens by homogeneous shear as material is advected through the pro-step-up shear zone.

The agreement between analogue and numerical model experiments and deformation patterns observed in small collisional orogens suggests that in these cases, crustal deformation may be controlled to first-order by subduction of mantle lithosphere. A number of comparisons between mantle subduction-driven models of collision and natural examples have been made (e.g. Beaumont et al. 1994; Batt and Braun 1997; Bousquet et al. 1997; Beaumont et al. 2000). Despite the success of some of these comparisons, the rheology used in the computer models is vastly simplified from real continental crust. Extrapolation of laboratory measurements to crustal strain rates is uncertain (Paterson 1987). The scale of the models and their inherent assumptions preclude the inclusion of small-scale heterogeneities explicitly; the layering of continental crust has also generally been neglected. Only recently have effects of strain localization, softening and hardening been considered (e.g. Cundall 1989; Mäkel and Walters 1993; Upton 1998; Vauchez et al. 1998; Schmid and Podlachikov 1999).

The models that were first used to highlight the importance of mantle lithosphere subduction (Malavieille 1984; Willett et al. 1993) used a one-layer frictional (Coulomb) representation of the crust. More complex rheologies, which combine rheologies representing the upper, brittle/frictional part of the crust with temperature-controlled viscous behaviour at depth, do not always show a strong crustal response to mantle lithosphere subduction boundary conditions (e.g. Royden 1996; Seyferth and Henk 2000). Further investigations are required to fully resolve the degree to which lower lithosphere dynamics control crustal deformation during collision.

Model properties

Figure 3 shows the boundary conditions and material properties used in the numerical model. As discussed above, the driving mechanism for collision is the assumed subduction of mantle lithosphere, represented in the model by a set of velocity boundary conditions at its base. The point S is a velocity discontinuity and represents the location of lower lithosphere detachment and underthrusting. To the left of S, the basal velocity is equal to the uniform convergence velocity of 1 cm a^{-1}, and to the right of S, the base of the crustal layer is fixed. Material properties in the model layers are followed using a Lagrangian tracking grid. The calculation is performed using an arbitrary Eulerian–Lagrangian formulation as described by Fullsack (1995).

The crustal rheology used in the model experiments is a combination of incompressible frictional Coulomb behaviour, with specified values for cohesion and internal angle of friction ϕ, and ductile power-law creep, specified in terms of a pre-exponential constant B, activation energy Q, and power-law exponent, n. In the frictional regime, shear strength increases with pressure following the Coulomb yield relationship $\tau=\tan(\phi)\ \sigma$ where τ and σ are the shear and normal stress, respectively, and the material has negligible cohesion. This yield strength with depth relationship approximates a uniform gradient form of Byerlee's Law (Byerlee 1978; Brace and Kohlstedt 1980) in a thrust environment for a fluid pressure slightly above hydrostatic. No account is taken of possible variations in fluid pressure ratios with depth (cf. Yardley and Valley 1997). In some of the experiments a simple representation of strain softening in the frictional regime is included. Given the uncertainties in representing strain softening and its effects, we model it in terms of a threshold bulk strain value, which produces a sudden decrease in Coulomb internal angle of friction by 60%.

Ductile strength obeys a power-law creep relationship $(\sigma_1-\sigma_3)=2B\,\dot{\epsilon}^{(1/n)}\exp(Q/n\mathrm{R}T)$, where $(\sigma_1-\sigma_3)$ is stress difference, $\dot{\epsilon}$ is strain-rate, R is the gas constant and T is temperature. The ductile creep parameters are based on results from laboratory deformation experiments, translated into values suitable for plane-strain calculations (Tullis et al. 1991). The transition between frictional plastic and ductile behaviour is dynamically determined in the models by the minimum calculated shear strength, and evolves in time and space (Fullsack 1995). The 'frictional-ductile' transition is a sharp boundary in the models, unlike in real continental rocks where rocks can be brittle on one spatial scale and ductile on another (e.g. Guermani and Pennacchioni, 1998; Herwegh et al. 1999).

The model experiments are designed to investigate the early stages of collision, where convergence rates (and the corresponding Péclet number, or ratio of heat advection to heat diffusion) are still high.

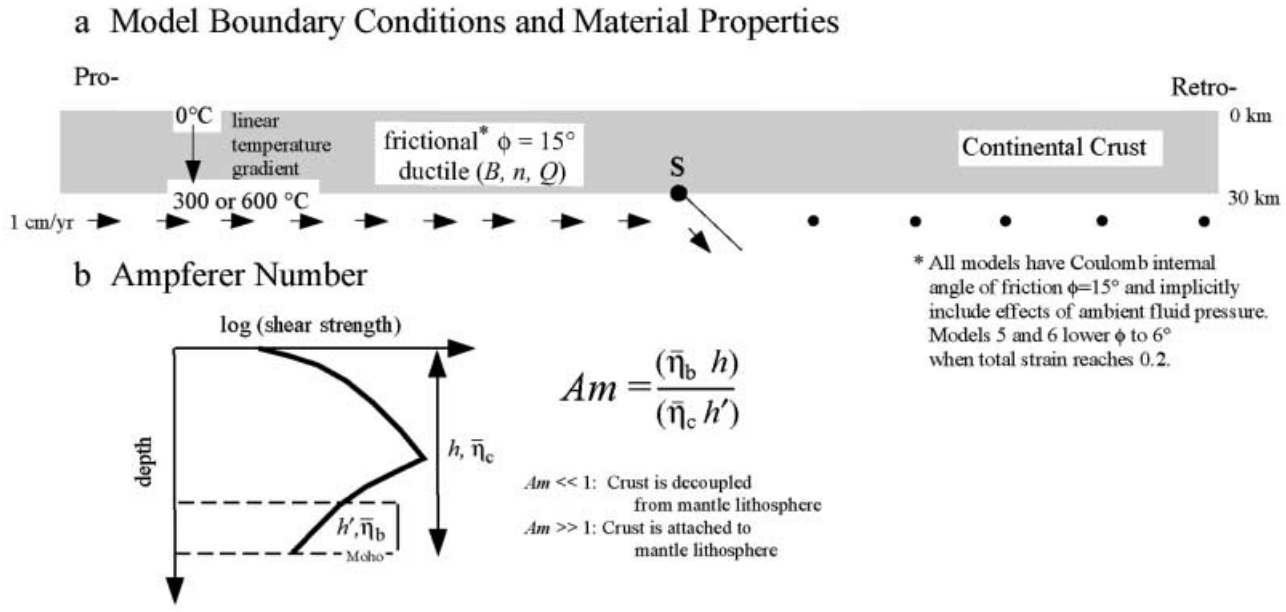

Fig. 3 Model properties. **a** Boundary conditions and rheology. *Lower arrows* and *dots* convergence of pro-mantle lithosphere and stationary retro-mantle lithosphere, respectively, separated by mantle subduction point *S*. One-layer crust has uniform frictional–viscous properties. Values for various model experiments are listed in Table 1. Translation factor between triaxial experimental constant A and plane-strain pre-exponential parameter B is $3^{(-(n+1)/2n)}\ 2^{((1-n)/n)}$ (after Tullis et al. 1991). Angle of internal friction in the Coulomb domain is lowered to implicitly include effects of fluid pressure. Initial geothermal gradient in the models is linear at 10 or 20 °C km^{-1}. **b** *Inset* showing definition of the non-dimensional Ampferer number (Am) as a function of the ratio of effective crustal viscosities in the crust for a typical crustal strength profile under compression (after Ellis 1996). Crustal thickness is h, and thickness of basal weak horizon is h'. Bulk average crustal viscosity and average viscosity of weak horizon, $\bar{\eta}_c$ and $\bar{\eta}_b$, are linearly averaged with depth over h and h', respectively, using true viscosity in ductile region and effective viscosity (shear stress $\tau/2\dot{\epsilon}$, where $\dot{\epsilon}$ is deviatoric strain rate) in frictional region, so that $\bar{\eta}_c = \frac{1}{h}\int_{z=-h}^{z=0} \eta dz$ and $\bar{\eta}_b = \frac{1}{h'}\int_{z=-h}^{z=h'-h} \eta dz$. h' is the thickness of a layer between the Moho and the depth at which viscosity η=(η_{Moho}×2.71). Am is computed for each vertical column of the model. In some of the experiments, Am is averaged horizontally to give an overall estimate, $\overline{Am}$.

Accordingly, the models have no thermal evolution, so that model material maintains the temperature assigned it at the start of an experiment. Linear geothermal gradients of either 10 °C km^{-1} (cold strong continental crust) or a more average gradient of 20 °C km^{-1} are used. The lack of thermal evolution means that results cannot be used to interpret thermally mature orogens such as the India–Eurasia collision, but may be relevant to the initial stages of collision in small orogens such as the Swiss Alps and the Pyrenees.

Erosion of surface topography is included in the sensitivity analysis for some of the model experiments. Erosion is modelled as a simple rate function proportional to the height of topography above base level (the initial model top surface), and sedimentation is neglected. For simplicity, thickening or thinning of the crust as a result of collision and/or erosion at the surface is not compensated flexurally as it would be in a real orogen. Instead, the base maintains a horizontal attitude. Isostatic compensation, if present, modifies the magnitude of the gravitational forces opposing crustal thickening (e.g. England and McKenzie 1982; Houseman and England 1986; Willett et al. 1993), but results are qualitatively similar.

Quantifying the effect of lower lithosphere subduction

If there are no localization processes operating within the crust, the degree to which the basal boundary condition influences deformation in the crustal layer above can be estimated quantitatively using the Ampferer number Am (Ellis et al. 1995; Ellis 1996). This number is the ratio between the far-field compressive forces or stresses operating on a contractional plate boundary, and the local shear forces or stresses transmitted from mantle lithosphere to the crust. It is similar to, and complements, another scaling number, the Argand number (England and McKenzie 1982; the ratio of gravitational force operating on thickened crust in an orogen to far-field compressive stresses). Am can be written in terms of a length-scale and viscosity ratio, where the length-scales may be derived from the boundary conditions or from inherent model behaviour. For model boundary conditions representing subduction of mantle lithosphere, there is no boundary length-scale, and the Ampferer number can be expressed in terms of the ratio of average crustal viscosity, $\bar{\eta}_c$, to the viscosity of the ductile low-strength channel just above the Moho, $\bar{\eta}_b$, scaled by the relative thickness of this channel (h') to the crust. Using

the expression from Fig. 3b, the Ampferer number may be directly computed for a given layer. Because effective viscosity depends on spatially varying strain-rate, Am will vary across the model domain and will change during evolution of the model orogen.

The magnitude of Am is solution-dependent, but gives a quantitative estimate of the coupling between crust and mantle lithosphere. If the crust has a very weak ductile channel at its base, which completely detaches it from the underlying mantle lithosphere, the average basal viscosity $\bar{\eta}_b \ll$ average crustal viscosity $\bar{\eta}_c$, and although the thickness of the weak horizon h' increases, $Am \ll 1$. For strong lower crust, no viscosity minimum occurs so that $h' \rightarrow 0, \bar{\eta}_c \approx \bar{\eta}_b$ and Am approaches infinity. As a result, cases with $Am \gg 1$ are strongly attached to underlying layers and exhibits the asymmetric deformation pattern characteristic of small collisional orogens. Provided the bulk strength of crust varies only slowly across strike, analysing behaviour in terms of the Ampferer number therefore gives a quantitative estimate of whether a model with a given set of material parameters, boundary conditions, and geothermal gradient will behave as predicted for small collisional orogens by previous studies (e.g. Malavieille 1984; Willett et al. 1993) or in a detached manner such as that generally only inferred for large, thermally evolved orogens.

Nominal results for a one-layer crust

The first two experiments shown (Figs. 4 and 5) are an illustration of the basic behaviours of a crustal layer under boundary conditions of mantle lithosphere subduction. Models 1 and 2 are identical, except that they have different initial geothermal gradients. Model 1 has a uniform geothermal gradient of $10\,^{\circ}\mathrm{C\ km^{-1}}$, corresponding to cold continental crust, and model 2 has a uniform geothermal gradient of $20\,^{\circ}\mathrm{C\ km^{-1}}$ representing continental crust with an average heat flow. Both experiments model the crust as one homogeneous layer with frictional strength ϕ=15° (lower than internal angles of friction normally used for crustal rocks, because this value implicitly takes effects of fluid pressure into account) and ductile properties corresponding to laboratory measurements for 'wet' diabase (Shelton and Tullis 1981) extrapolated to crustal temperatures and pressures and for plane-strain conditions. We use the term 'wet' to mean that the sample was dried at a low to moderate temperature, so that hydrous mineral phases were still present.

Figure 4 shows the main features of model 1 at the onset of collision (Fig. 4a–c) and after 100 km of convergence (Fig. 4d). Strength profiles (Fig. 4a) indicate that crust is so cold that it remains in the frictional regime down to its base. Focused uplift and deformation above point S (Fig. 4b) results directly from forcing by the asymmetric mantle lithosphere subduction below. The Ampferer number is very high across the model domain, showing that the strong crustal base remains well-coupled to its basal boundary condition (Fig. 4c). After 100 km of convergence, a large, focused plug with pro- and retro-wedges on either side has formed directly above S (Fig. 4d). Despite the lack of erosion and isostatic compensation in this model, the asymmetric style of deformation and focused thickening patterns are in first-order agreement with those observed at collisional orogens such as the Alps. However, the strength profiles are quite unlike those predicted using normal crustal geotherms and experimental flow-law data (cf. Fig. 1).

Model 2 (Fig. 5) is the same as model 1 except that it has a higher geothermal gradient. As a result, the base of the model crust deforms in the ductile regime (Fig. 5a). Uplift is much less focused, and strain rates are high within a ductile channel next to the Moho (Fig. 5b). The Ampferer number is <1, indicating that crust is partially decoupled from underlying lithosphere (Fig. 5c). After 100 km convergence the result of this diffuse deformation is distributed thickening over a wide zone on either side of the S point (Fig. 5d), with a thin basal layer that has opposite shear sense on pro- and retro-sides.

These simple experiments show a potential difficulty in the interpretation of 'Christmas tree' strength profiles in terms of crustal dynamics. Model 1 has a very cold continental geotherm and strength profiles are stronger than those computed using more reasonable heat-flow and material properties (e.g. Fig. 1). Yet the dynamics of this experiment correspond much more closely to those inferred for small collisional orogens [e.g. European Alps (Pfiffner 1992); Pyrenees (Muñoz 1992); New Zealand Southern Alps (Walcott 1998)] than the dynamics of model 2. This model, which has a more typical continental geotherm, has strength profiles similar to those shown in Fig. 1, but its dynamics correspond much more closely to the dynamics of large orogens such as the Tibetan Plateau, interpreted to be thermally mature (e.g. Houseman and England 1986; Royden 1996) than to small collisional orogens.

Some of the previous studies that have investigated collisional dynamics using numerical models have avoided this problem by using only a frictional representation of the crust (e.g. Willett et al. 1993). Whenever ductile properties of lower crust based on laboratory experiments are used, however, crustal temperatures must be kept unnaturally low (e.g. Beaumont et al. 1994), or the ductile strength of the lower crust has to be increased by at least an order of magnitude (e.g. Ellis et al. 1999; Seyferth and Henk 2000) to avoid decoupling like that seen in model 2. Since the diffuse style of thickening in this model is only observed in large hot orogens, these discrepancies suggest that something in the model representations is not correct. Either the extrapolation of laboratory ductile flow-law data to lower crustal conditions is an underestimate of true rheological strength, so that a

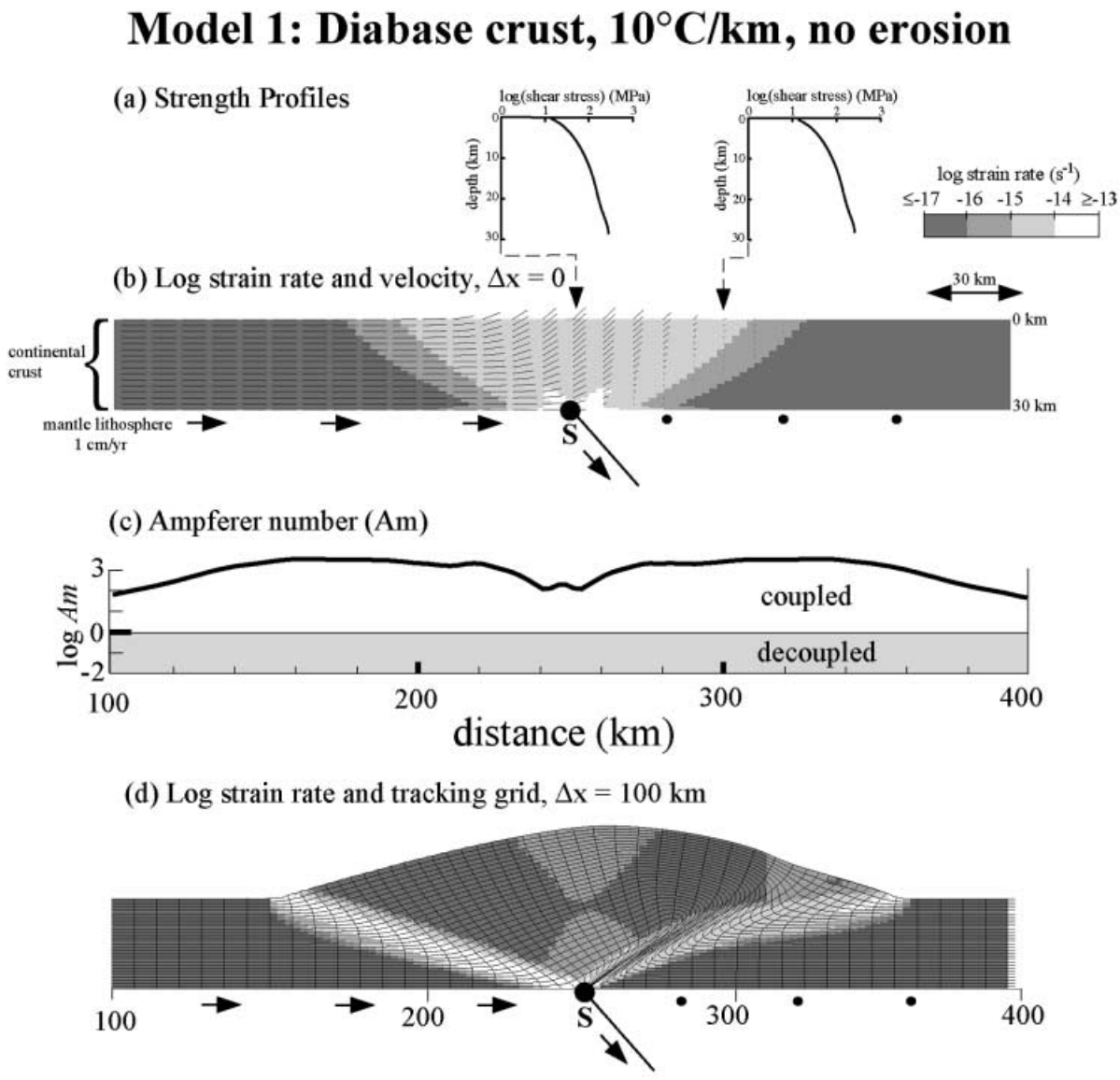

Fig. 4 Model 1, showing continental collision forced by mantle lithosphere subduction for cold, one-layer continental crust. Geothermal gradient is 10 °C km^{-1}, frictional strength ϕ=15°, and ductile material values are wet diabase (Shelton and Tullis 1981). **a** Two selected strength profiles for vertical sections indicated by *dashed lines* on **b**. Strong cold crust remains frictional down to its base. **b** Second invariant of the deviatoric strain rate tensor (*shading*) and velocity vectors (*lines*) for convergence Δx=0 km. Maximum vector length corresponds to a velocity of 1 cm a^{-1}. *Large black dot* is the velocity discontinuity point *S*. Note step-up shear zones on either side of point *S*, and plug uplift of crust between them. **c** Ampferer number as a function of horizontal location matching **b**, showing zone in which crust is strongly coupled to mantle lithosphere (log Am>0). **d** Strain rate and tracking grid after Δx=100 km convergence for model 1. Note the outward rotation of the pro- and retro-step-up shear zones as a result of the development of topography

strength minimum does not occur at the base of the crust, or the boundary conditions and rheology used in model 2 are insufficient to reproduce dynamics of real collisional orogens. In the next section, we conduct a series of sensitivity analyses to establish various factors that may explain this discrepancy.

A preliminary sensitivity analysis

Sensitivity to material properties

Representation of lower crustal rocks by a uniform layer with ductile properties based on one predominant mineral or rock-type is obviously a simplification of the true complexity of lower crustal rheology. To test the effect of using a variety of flow-law data, we ran a series of experiments similar to those shown in models 1 and 2 (Figs. 4 and 5) for flow-law data for other mineral or rock compositions (Table 1). For simplicity we only investigated behaviour for a homogeneous one-layer crust at two geothermal gradients. Crust that contains two or more layers separated by weak ductile detachments behaves in a

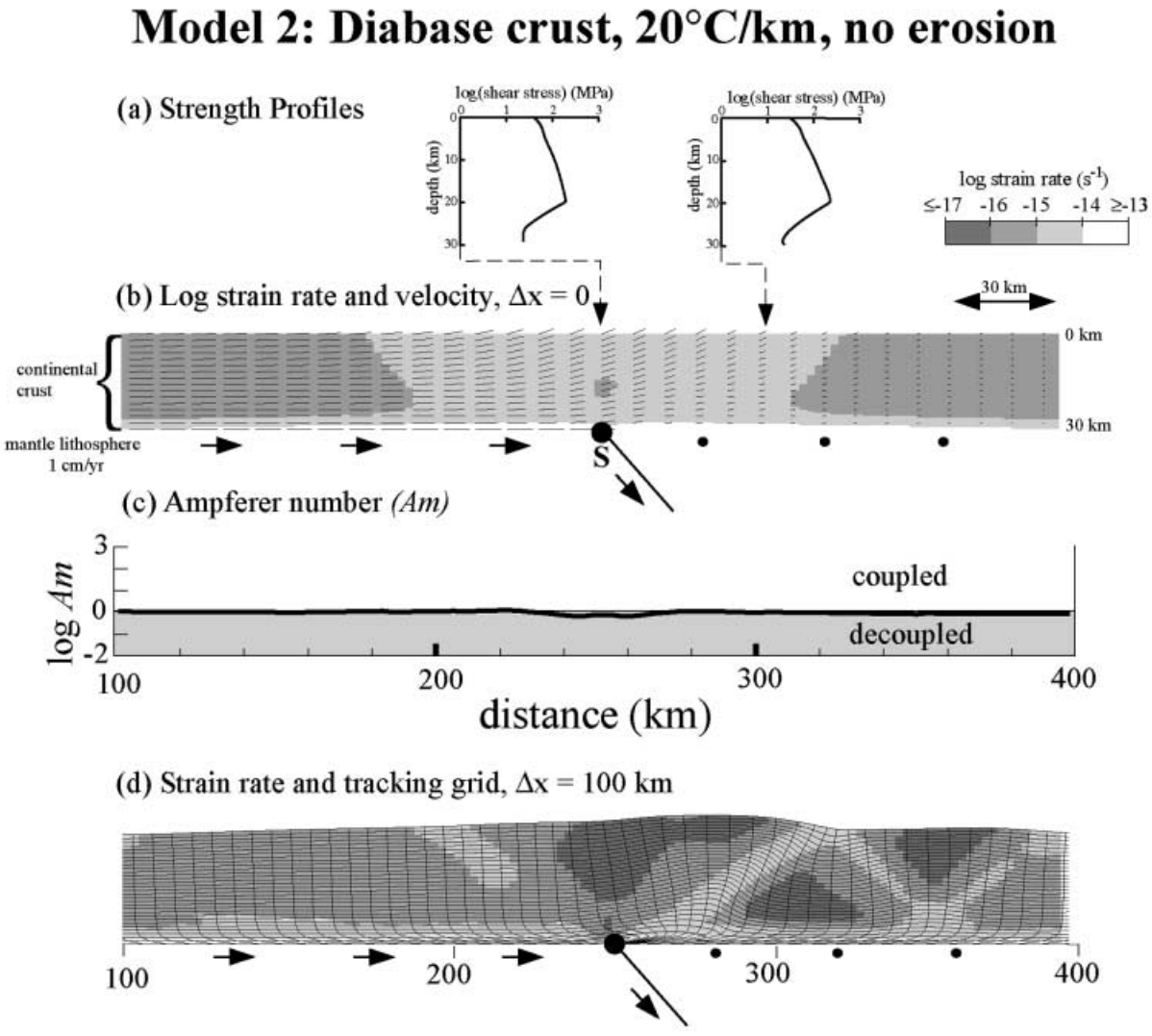

Fig. 5 Model 2, the same as the previous experiment except with a linear geothermal gradient of 20 °C km^{-1}, representing an average continental geotherm. Panels are equivalent to those shown in Fig. 4, and show a much broader, diffuse style of deformation in **a** strength profiles, which show a weak ductile minimum at the base of the crust; **b** strain rates and velocities, which show maximum strain rates along a weak zone at the base of the crust; **c** log Am<0, indicating crust decoupled from mantle lithosphere; and **d** finite convergence of Δx=100 km, showing thickening over a wide zone on either side of mantle subduction point S

more complex manner (e.g. Beaumont and Quinlan 1994; Batt and Braun 1997), but still preserves a signature of mantle lithosphere subduction, if coupling between lower crust and mantle lithosphere is strong.

Figure 6 shows the result of the sensitivity analysis in a plot of the Ampferer number averaged across strike versus mineral type for geothermal gradients of 10 °C km^{-1} (squares) and 20 °C km^{-1} (polygons). Polygons with arrows have Am approaching infinity, which occurs when no strength minimum occurs at the base of the crust. The exact Am values in these cases are not significant, but indicate that crust is strongly coupled to underlying mantle lithosphere. A variety of crustal mineral and rock types were selected for the analysis, as well as one mantle lithosphere mineral (wet olivine; Table 1). Most laboratory experiments on lower crustal rocks have been carried out on using 'wet' samples containing hydrous phases (e.g. Shelton and Tullis 1981), whereas samples dried at high temperatures are generally much stronger (e.g. Mackwell et al. 1998). We have included both wet and dry data in our sensitivity study to indicate how lower crustal strength may vary by several orders of magnitude depending on whether hydrous or dry conditions are present.

The sensitivity analysis clearly demonstrates that strong crust–mantle lithosphere coupling (log Am >0) only occurs for cold continental crust, for ultramafic rocks, or for rheology based on dry rock samples. Minerals that are normally inferred to be dominant for lower crustal compositions (hydrous feldspar, clinopyroxene and diabase) exhibit decoupled behaviour for more typical geothermal gradients of 20 °C km^{-1}.

Table 1 Model flow-law parameter values investigated. Power-law ductile flow-law: $(\sigma_1 - \sigma_3) = 2B\,\dot{\varepsilon}^{(1/n)} \exp(Q/nRT)$ where $(\sigma_1$–$\sigma_3)$ is stress difference, $\dot{\varepsilon}$ deviatoric strain-rate; B pre-exponential constant for plane-strain; Q activation energy; n power-law exponent; R gas constant; T temperature. The translation factor between triaxial experimental constant A and plane-strain pre-exponential constant B is $3^{(-(n+1)/2n)}2^{((1-n)/n)}$ (Tullis et al. 1991)

Mineral/rock type	A ($MPa^{-n}\,s^{-1}$)	Q ($kJ\,mol^{-1}$)	n	B ($MPa\,s^{1/n}$)	Source
Quartz (wet)	2.91×10^{-3}	151	1.8	8.018	Jaoul et al. (1984)
Feldspar (wet)	3.27×10^{-4}	238	3.2	3.710	Shelton and Tullis (1981)
Diabase (wet)	2.02×10^{-4}	259	3.4	3.677	Shelton and Tullis (1981)
Diabase (dry)	8.00×10^{0}	485	4.7	0.191	Mackwell et al. (1998)
Pyroxene (wet)	1.58×10^{1}	335	2.5	0.101	Shelton and Tullis (1981)
Olivine (wet)	4.20×10^{2}	498	4.48	0.077	Chopra and Paterson (1981)

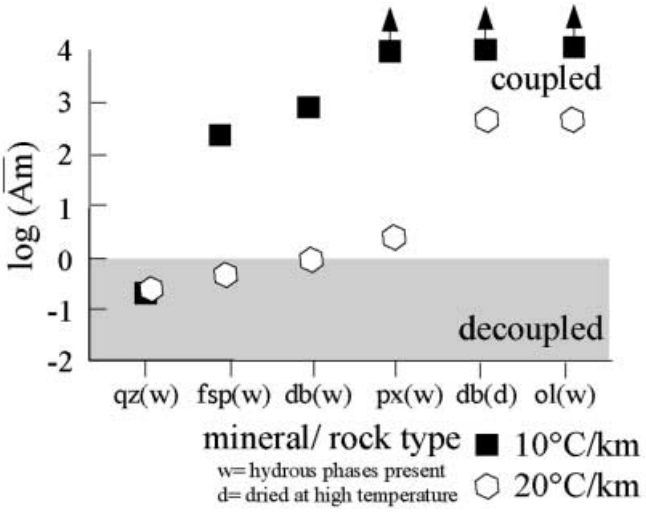

Fig. 6 A sensitivity analysis, using ductile material constants based on different assumed mineral compositions for a one-layer crust. Results are shown for cold crust (10 °C km^{-1}, *squares*) and crust with an average continental geotherm of 20 °C km^{-1}, *hexagons*). *qz* Quartz; *fsp* feldspar; *db* diabase; *px* pyroxene; *ol* olivine; where material parameters in each case are taken from the sources shown in Table 1. *w* and *d* refer to hydrous and dry samples, respectively, where '*dry*' means dried at a high temperature. *Arrows on upper squares* indicate values for log *Am* that are so large that they plot out of range of figure

Unless flow-law parameters from laboratory measurements strongly underestimate strength of the lower crust, other effects must be responsible for the model discrepancy. We investigate some of these effects below.

Sensitivity to erosion

Model experiments 1 and 2 and those summarized in Fig. 6 have no erosion of surface topography. Erosion has been shown to have a major effect on the style of continental dynamics in other model studies (e.g. Beaumont et al. 1992; Willett 1999). Figure 7 illustrates the effect of erosion in a comparison between three experiments with negligible, moderate, or near total erosion of topography after 100 km of convergence. The model shown in Fig. 7a is the same as model 2 (Fig. 5), but this time the position of the frictional–ductile transition (dashed line on upper panel) and the total strain (lower panel) are illustrated.

The contrast between the cases with no and near total erosion is apparent (Fig. 7a versus c). Exhumation of uplifted material in the latter experiment advects isotherms upwards near the *S* point and, as a result, the strain becomes more localized in the core of the orogen with increasing convergence. This creates a crustal-scale shear zone rooting into *S* and suppressing detachment of model lower crust like that seen in Fig. 7a. Total strain near *S* is high, and the frictional–ductile transition is very close to the surface. Although these models have no thermal evolution, Fig. 7c (model 4) indicates that when rates of compression and erosion are high in comparison to the characteristic thermal relaxation time, elevated temperatures, heat flow and ductile flow will occur very close to the surface. Similar model experiments that include thermal evolution also show this effect (Batt and Braun 1997). The results for moderate erosion (Fig. 7b, model 3) are intermediate in terms of the degree of detachment of lower crust from mantle lithosphere and the extent of crustal deformation, but still clearly show the role of erosion in focusing strain, especially within the upper (frictional) crust.

The effect of erosion is a form of inherent localization resulting from the upward advection of isotherms. Strength profiles for two positions on either side of *S* (Fig. 7) demonstrate how the 'Christmas trees' predicted using dynamic models are more heterogeneous as a function of position for higher rates of erosion and exhumation. Because samples of lower crust are often taken from regions that have experienced orogenic activity and that show pervasive ductile deformation, the contrast between strength profiles over a distance of only 30 km (e.g. Fig. 7c) indicate that strength estimates for lower crust derived from these rocks may not be representative for lower crust in general, and that large variations in strength are to be expected as a result of the deformation and localized exhumation (Royden 1998).

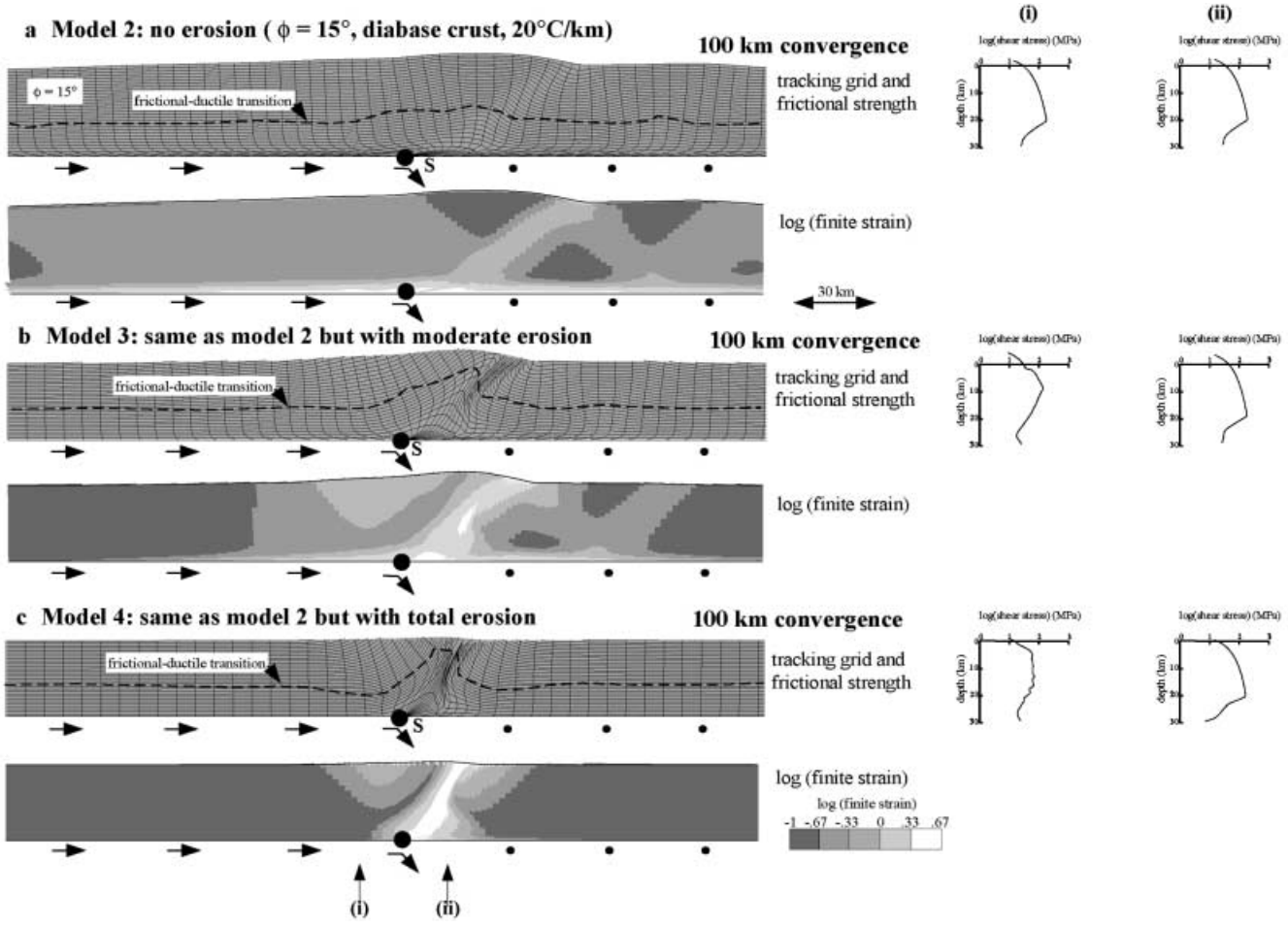

Fig. 7 Comparison between models with different amounts of erosion after 100 km convergence. All have a one-layer crust with frictional strength ϕ=15°, wet diabase ductile properties, and a geothermal gradient of 20 °C km^{-1}. **a** Model 2 (as for Fig. 5), showing tracking grid with the frictional-ductile transition (*dashed line*) superimposed. Lower panel shows log (total strain). No erosion creates excess topography and trigger detachment between crust and lower layers (high strain zone at base of crust). **b** Same as model 2 but with moderate erosion of topography proportional to base level. **c** Same as model 2 but for near total erosion of topography. The upward deflection of the frictional-ductile transition near the mantle subduction point *S* is accompanied by a zone of high strain. Style of deformation is very asymmetric, with strain concentrated along the retro-step-up shear zone. All three models have two representative strength profiles shown at side, where vertical co-ordinate is depth relative to position of initial (unthickened) model surface. (Location of profiles indicated by *vertical arrows* and *roman numerals* at bottom of figure)

Sensitivity to strain localization in the upper crust

Strain localization may also occur as a result of rheological strength changes during deformation. For example, high strain zones within the frictional domain may experience a reduction in strength (strain softening) because of fluid weakening, dilatancy or other rheological changes. Strain softening during ductile deformation may occur because of grain size changes and/or changes in deformation mechanisms. Although the relationship between material softening/hardening and localization and its significance for bulk crustal strength is not clear and is the topic of ongoing research (e.g. Jin et al. 1998; de Bresser et al. 1999; Hobbs et al. 1999; Rubie et al. 1999), we present one simple example to illustrate the effects of localization resulting from strain softening. We have chosen an arbitrary approach where frictional strength is reduced suddenly at a strain threshold of 0.2, from the nominal value of 15° to 6°. The area with reduced frictional strength is shown on the upper panels of the model experiment (Fig. 8) after 50 and 100 km convergence.

Two observations are immediately apparent when comparing the result of model 5 with the case with no strain softening (model 2, Fig. 5). First, the position of the frictional–ductile transition is deflected downwards within the strain-softened region, because frictional yield strength is reduced. Second, strain is much more focused than for the case with no strain softening. Rather than a continuous pro-shear zone, which gradually thickens crust in a distributed manner, the shear zone remains focused within a strain-softened region until advection of material retro-wards causes shear to jump into incoming undeformed pro-crust. This

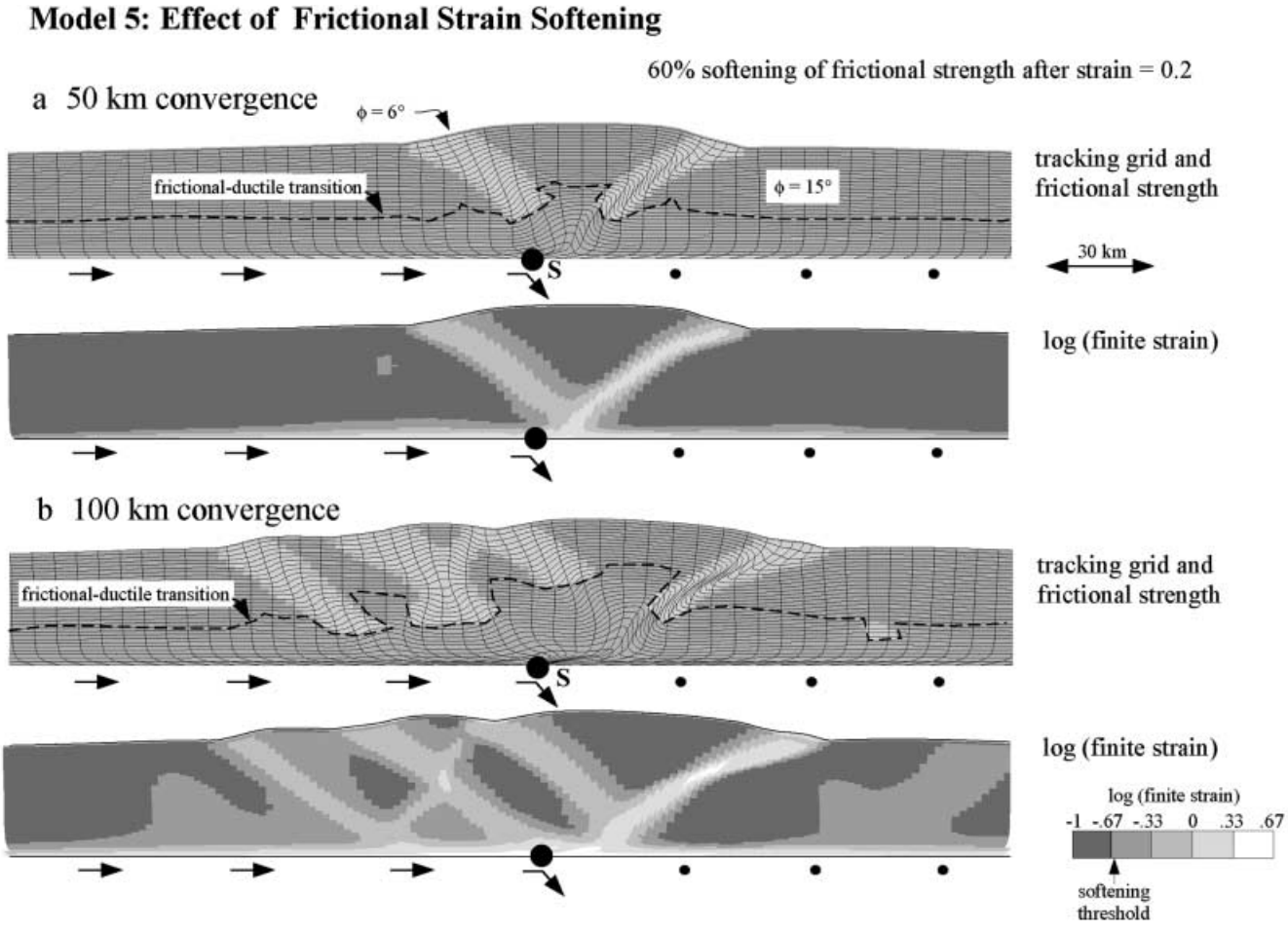

Fig. 8 A model demonstrating the effect of frictional strain softening. All other parameters are identical to model 2 (Fig. 5), and there is no erosion. An arbitrary strain softening after strain reaches value 0.2 reduces the internal angle of friction from 15° to 6°. Area of strain softening is indicated by unshaded region on upper panels after **a** 50 km and **b** 100 km convergence. The lower panel in each case shows log (total strain). Grid and strain plots show a progressive jumping of the pro-shear zone away from the model orogen as material is advected towards *S*. Strain is highest on the base and retro-step-up shear zone. The frictional–ductile transition is deflected downwards within the strain-softened areas

creates an episodic thrust style, similar to that observed for sandbox experiments with a weak base (e.g. Mulugeta 1988) and in numerical models which have included effects of dilatation, cohesion and strain softening (e.g. Mäkel and Walters 1993; Sassi and Faure 1997). Retro-shear remains focused in the same region, where deformation becomes relatively localized. Although some detachment between crust and underlying layers still occurs, the deformation is much more focused above *S* than for model 2, and it would be easier to distinguish the mantle subduction signature within the crust in this case.

The effect of strain softening combined with moderate erosion is capable of producing an even more focused model orogen (model 6; Fig. 9). In this case, the outward stepping of the pro-shear zone caused by the effects of thickened crust is suppressed. Instead, an intense retro-shear zone develops along which lower crustal material is exhumed at the surface. Crust–mantle detachment is also suppressed compared with models 2 and 5. Because the model does not include thermal equilibration, the frictional–ductile transition is almost exposed at the surface after 100 km convergence.

Discussion and conclusions

The asymmetric, focused plug uplift seen in small collisional orogens such as the Swiss Alps has been explained by previous studies as a direct result of motion in the underlying mantle lithosphere (e.g. Malavieille 1984; Willett et al. 1993). However, we have shown that for average continental geotherms, model lower crust with ductile flow parameters taken from laboratory experiments will detach from underlying mantle lithosphere and will not form a focused region of uplift, unless some localization factor is present. In the Alps, lower crust remained attached to mantle lithosphere and has been subducted. Upper

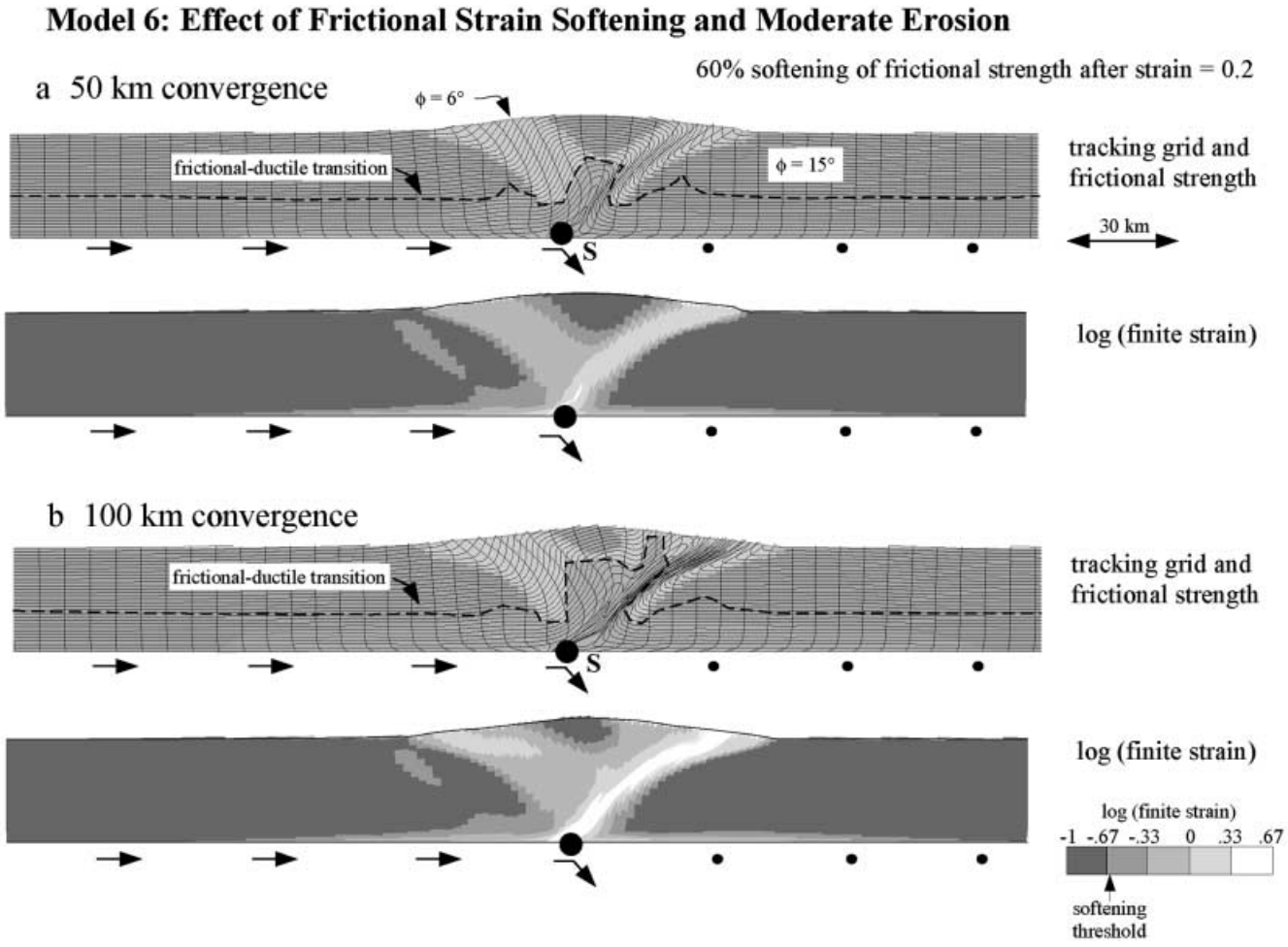

Fig. 9 The combined effect of frictional strain softening and moderate erosion of topography proportional to height above base level. The experiment is otherwise identical to model 2 (Fig. 5). Upper panels show grid and frictional–ductile transition, and lower panels log (total strain), after **a** 50 km, and **b** 100 km convergence. Frictional–ductile transition is progressively advected towards surface. Strain is more focused than for the moderate erosion case with no frictional strain softening (Fig. 7b)

crust detached, but does not exhibit diffuse straining as seen in model 2 (with no denudation). Instead, upper crust deformed in a localized fashion like models that include denudation (e.g. model 4) and/or other forms of strain localization (e.g. models 5 and 6).

Comparison between observations and these simple models suggest that either extrapolation of laboratory measurements for lower crustal minerals and rocks to crustal conditions underestimates average strength of lower crust, or focused plug uplift is not only a result of lower lithosphere subduction, but rather caused by a combination of underthrusting of lower lithosphere and other factors that promote localization. As in previous studies, we suggest that denudation plays a major role in the preservation of mantle subduction signature in the crust. Further, we suggest that if current estimates of lower crustal rock strengths are correct so that a strength discontinuity is present at or near the Moho, Alpine-style orogens would not exist without the presence of syn-tectonic erosion and strain localization. Collisional plate boundaries would instead be diffuse zones of crustal thickening with little surface expression.

Acknowledgements This study was inspired by the workshop on rheology and geodynamic modelling organized by Georg Dresen and Mark Handy. We would like to thank them for encouraging us to examine this problem. Research was funded by Swiss National Foundation grant 20-43246.95 to A.P. Constructive reviews by Georg Dresen and Mervyn Paterson helped to improve the manuscript, and Chris Beaumont provided many useful ideas and information on the use of laboratory creep data in plane-strain models. We would also like to thank Andreas Henk, Marco Herwegh, Stefan Schmid, Michael Seyferth and Olivier Vanderhaeghe for discussions and encouragement.

References

Albert RA, Phillips RJ, Dombard AJ, Brown CD (2000) A test of the validity of yield strength envelopes with an elasto-viscoplastic finite element model. Geophys J Int 140:399–409.

Batt G, Braun J (1997) On the thermo-mechanical evolution of compressional orogens. Geophys J Int 128:364–382

Beaumont C, Fullsack P, Hamilton J (1992) Erosional control of active compressional orogens. In: McClay KR (ed) Thrust tectonics. Chapman and Hall, London, pp 1–18

Beaumont C, Quinlan G (1994) A geodynamic framework for interpreting crustal-scale seismic-reflective patterns in compressional orogens. Geophys J Int 116:754–783

Beaumont C, Fullsack P, Hamilton J (1994) Style of crustal deformation caused by subduction of the underlying mantle. Tectonophysics 232:119–132

Beaumont C, Muñoz JA, Hamilton J, Fullsack P (2000) Factors controlling the Alpine evolution of the Central Pyrenees inferred from a comparison of observations and geodynamical models. J Geophys Res 105:8121–8145

Bousquet R, Goffé B, Henry P, Le Pichon X, Chopin C (1997) Kinematic, thermal and petrological model of the Central Alps: Lepontine metamorphism in the upper crust and eclogitisation of the lower crust. Tectonophysics 273:105–127

Brace, WF, Kohlstedt, JL (1980) Limits on lithospheric stress imposed by laboratory experiments. J Geophys Res 85:6248–6252

Byerlee JD (1978) Friction of rocks. Pure Appl Geophys 116:615–626

Chopra PN, Paterson MS (1981) The experimental deformation of dunite. Tectonophysics 78:453–473

Cundall P (1989) Numerical experiments on localisation in frictional materials. Ingenieur-Archiv 59:148–159

de Bresser J, ter Heege J, Spiers C (1999) Grain size reduction by dynamic recrystallization: can it result in major rheological weakening? (Abstract) In: Dresen G, Handy M, Janssen C (eds) Deformation mechanisms, rheology and microstructures conference, 22–26 March 1999, Neustadt-an-der-Weinstrasse. GeoforschungsZentrum and the Justus-Liebig-Universität, Potsdam, p 17

Ellis S (1996) Forces driving continental collision: reconciling indentation and mantle subduction tectonics. Geology 24:699–702

Ellis S, Beaumont C, Fullsack P (1995) Oblique convergence of the crust driven by basal forcing: implications for length-scales of deformation and strain partitioning in orogens. Geophys J Int 120:24–44

Ellis S, Beaumont C, Quinlan G, Jamieson R (1999) Continental collision including a weak zone – the vise model and its application to the Newfoundland Appalachians. Can J Earth Sci 35:1323–1346

England P, McKenzie D (1982) A thin viscous sheet model for continental deformation. R Astron Soc Geophys J 70:295–321

Fullsack P (1995), An arbitrary Lagrangian–Eulerian formulation for creeping flows and applications in tectonic models. Geophys J Int 120:1–23

Guermani A, Pennacchioni G (1998) Brittle precursors of plastic deformation in a granite: an example from the Mont Blanc massif (Helvetic, western Alps). J Struct Geol 20:135–148

Handy MR, Wissing SB, Streit JE (1999) Frictional-viscous flow in mylonite with varied bimineralic composition and its effect on lithospheric strength. Tectonophysics 303:175–191

Herwegh M, Pfiffner OA, Kunze K (1999) Dynamic recrystallisation of carbonate mylonites at the brittle-plastic transition: evidence from the Helvetic Nappes (Abstract) In: Dresen G, Handy M, Janssen C (eds) Deformation mechanisms, rheology and microstructures conference, 22–26 March 1999, Neustadt-an-der-Weinstrasse. GeoforschungsZentrum and the Justus-Liebig-Universität, Potsdam, p 22

Hobbs B, Ord A, Mühlhaus H (1999) Strain localisation (Abstract). In: Dresen G, Handy M, Janssen C (eds) Deformation mechanisms, rheology and microstructures conference, 22–26 March 1999, Neustadt-an-der-Weinstrasse. GeoforschungsZentrum and the Justus-Liebig-Universität, Potsdam, p 23

Houseman G, England P (1986) Finite strain calculations of continental deformation; 1, Method and general results for convergent zones. J Geophys Res 91:3651–3663

Jaoul O, Tullis J, Kronenberg A (1984) The effect of varying water contents on the creep behavior of Heavitree quartzite. J Geophys Res 89:4298–4312

Jin D, Karato S-I, Obata M (1998) Mechanisms of shear localization in the continental lithosphere: inference from the deformation microstructures of peridotites from the Ivrea zone, northwestern Italy. J Struct Geol 20:195–209

Kohlstedt, DL, Evans B, Mackwell SJ (1995) Strength of the lithosphere: constraints imposed by laboratory experiments. J Geophys Res 100:17587–17602

Mackwell SJ, Zimmerman ME, Kohlstedt DL (1998) High-temperature deformation of dry diabase with application to tectonics on Venus. J Geophys Res 103:975–984

Mäkel G, Walters J (1993) Finite-element analyses of thrust tectonics: computer simulation of detachment phase and development of thrust faults. Tectonophysics 226:167–185

Malavieille J (1984) Modélisation expérimentale des chevauchements imbriqués: application aux chaînes des montagnes. Bull Soc Geol Fr 26:129–138

Mulugeta G (1988) Modelling the geometry of Coulomb thrust wedges. J Struct Geol 10:847–859

Muñoz JA (1992) Evolution of a continental collision belt: ECORS-Pyrenees crustal balanced cross section. In: McClay K (ed) Thrust tectonics. Chapman and Hall, New York, pp 235–246

Okaya N, Cloetingh S, Mueller St (1996) A lithospheric cross section through the Swiss Alps (Part II): constraints on the mechanical structure of a continent-continent collision zone. Geophys J Int 127:399–414

Paterson MS (1987) Problems in the extrapolation of laboratory rheological data. Tectonophysics 133:33–43

Pfiffner OA (1992) Alpine orogeny. In: Blundell D, Freeman R, Mueller S (eds) A continent revealed: the European geotraverse. Cambridge University Press, Cambridge, pp 180–190

Pfiffner OA, Heitzmann P (1997) Geologic interpretation of the seismic profiles of the Central Traverse (lines C1, C2, C3-north). In: Pfiffner OA, Lehner P, Heitzmann P, Mueller S, Steck A (eds) Deep structure of the Swiss Alps: results of NRP 20. Birkhäuser Verlag, Basel, pp 115–122

Pfiffner OA, Hitz L (1997) Geologic interpretation of the seismic profiles of the Eastern Traverse (lines E1-E3, E7-E9): eastern Swiss Alps). In: Pfiffner OA, Lehner P, Heitzmann P, Mueller S, Steck A (eds) Deep structure of the Swiss Alps: results of NRP 20. Birkhäuser Verlag, Basel, pp 73–100

Ranalli G, Murphy DC (1987) Rheological stratification of the lithosphere. Tectonophysics 132: 281–295

Royden L (1996) Coupling and decoupling of crust and mantle in convergent orogens; implications for strain partitioning in the crust. J Geophys Res 101:17679–17705

Royden L (1998) Geological insights into the deep crust; what can the upper crust tell us about what's underneath? (Abstract) Geol Soc Am 1998 Annual Meeting. Geol Soc Am 30:243

Rubie D, Mosenfelder J, Kerschhofer L (1999) Rheological weakening caused by mineral reactions (Abstract). In: Dresen G, Handy M, Janssen C (eds) Deformation mechanisms, rheology and microstructures conference, 22–26 March 1999, Neustadt-an-der-Weinstrasse. Geoforschungs-Zentrum and the Justus-Liebig-Universität, Potsdam, p 41

Sassi W, Faure J-L (1997) Role of faults and layer interfaces on the spatial variation of stress regimes in basins: inferences from numerical modelling. Tectonophysics 266: 101–119

Schmid D, Podladchikov Yu (1999) Modeling of strain softening as a function of microstructural heterogeneity (Abstract) In: Dresen G, Handy M, Janssen C (eds) Workshop on rheology and geodynamic modeling, conference on deformation mechanisms, rheology and microstructures. Geoforschungszentrum, Potsdam, p 45

Schmid SM (1999) What does nature tell us about rock rheology? (Abstract). In: Dresen G, Handy M, Janssen C (eds) Workshop on rheology and geodynamic modeling, conference on deformation mechanisms, rheology and microstructures. 22–26 March 1999, Neustadt-an-der-Weinstrasse. Geoforschungszentrum and the Justus-Liebig-Universität, Potsdam, p 165

Seyferth M, Henk A (2000) Deformation, metamorphism and exhumation-quantitative models for a continental collision zone in the Variscides. In: Franke W, Haak V, Oncken O, Tanner D (eds) Orogenic processes: quantification and modelling in the Variscan Belt. Geol Soc Lond Spec Publ, 179:217–230

Shelton G, Tullis J (1981) Experimental flow laws for crustal rocks (abstract) Eos Trans Am Geophys Union 62:396

Tullis TE, Horowitz FG, Tullis J (1991) Flow laws of polyphase aggregates from end-member flow laws. J Geophys Res 96:8081–8096

Upton P (1998) Modelling localization of deformation and fluid flow in a compressional orogen; implications for the Southern Alps of New Zealand. Am J Sci 4:296–323

Vauchez A, Tommasi A, Barruol G (1998) Rheological heterogeneity, mechanical anisotropy and deformation of the continental lithosphere. Tectonophysics 296:61–86

Walcott R (1998) Modes of oblique compression: Late Cenozoic tectonics of the South Island of New Zealand. Rev Geophys 36:1–26

Willett SD (1999) Orography and orogeny: the effects of erosion on the structure of mountain belts. J Geophys Res 104:28957–28981

Willett S, Beaumont C, Fullsack P (1993) A mechanical model for the tectonics of doubly vergent compressional orogens. Geology 21:371–374

Yardley BWD, Valley JW (1997) The petrologic case for a dry lower crust. J Geophys Res 102:12173–12185

Ye S (1992) Crustal structure beneath the Central Swiss Alps derived from seismic refraction data, unpublished. PhD Thesis 9631, ETH Zürich